Supporting Information

Effect of the Graphene Integration Process in the Performance of Graphene-based Schottky Junction Solar Cells

*Yunseong Choi,‡ Junghyun Lee,‡ Jihyung Seo,‡ Seungon Jung, Ungsoo Kim, and Hyesung Park**

Department of Energy Engineering, School of Energy and Chemical Engineering, Low Dimensional Carbon Materials Center, Perovtronics Research Center, Ulsan National Institute of Science and Technology (UNIST), Ulsan 44919, Republic of Korea

*Corresponding author

Email address: hspark@unist.ac.kr

Contents:

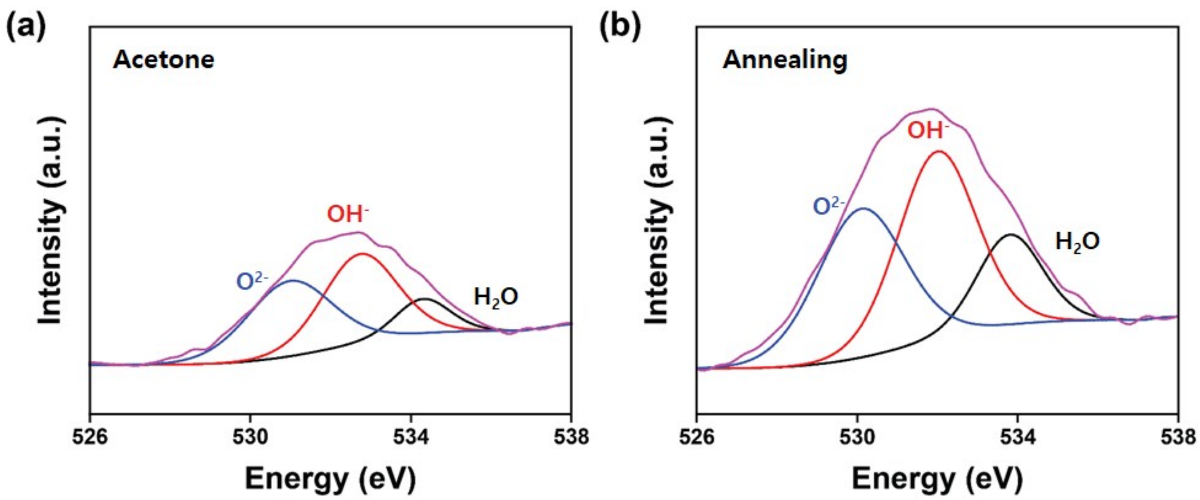

Fig. S1 XPS spectra of acetone- and annealing-transferred graphene. The O 1s XPS spectra of (a) acetone-transferred graphene and (b) annealing-transferred graphene indicate that the doping effect from the oxygen-derived materials is more pronounced on the surface of annealing-treated graphene.

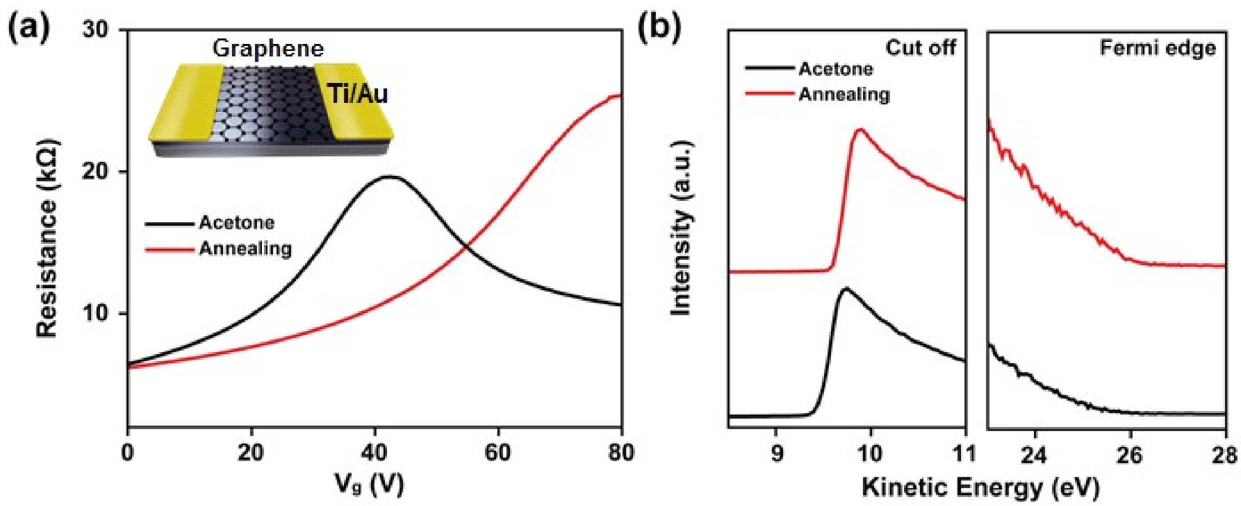

Fig. S2 Effect of different PMMA removal approaches on the doping level in graphene analyzed from transport and UPS measurements. (a) Transport measurements of graphene-based FETs processed with acetone and annealing treatments (Insert: Schematic diagram of graphene-FET). (b) UPS measurements of graphene films processed with acetone and annealing treatments.

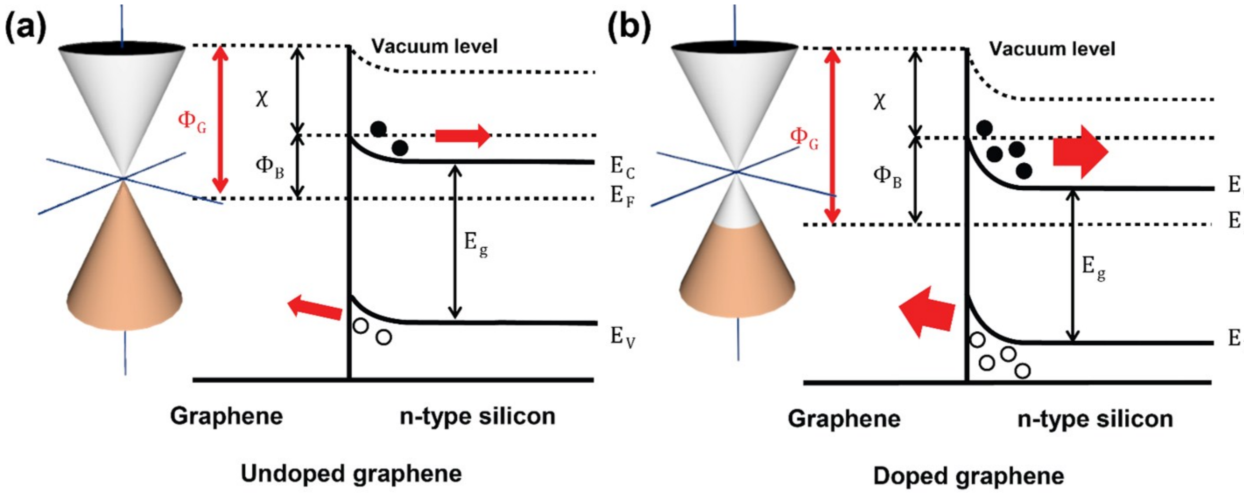

Fig. S3 Schematic energy band diagram of graphene-silicon Schottky junction with different doping level in graphene. (a) Energy band diagram of undoped graphene and silicon heterojunction. Holes (empty circles) and electrons (filled circles) are separated and collected toward the graphene and counter electrode, respectively. (b) Energy band diagram of hole doped graphene and silicon heterojunction. Hole doping increases the work function of graphene and Schottky barrier height, which enhances the built-in potential. The increased built-in potential then promotes the photogenerated charge separation and collection more effectively in doped graphene-silicon junction compared to the undoped case.

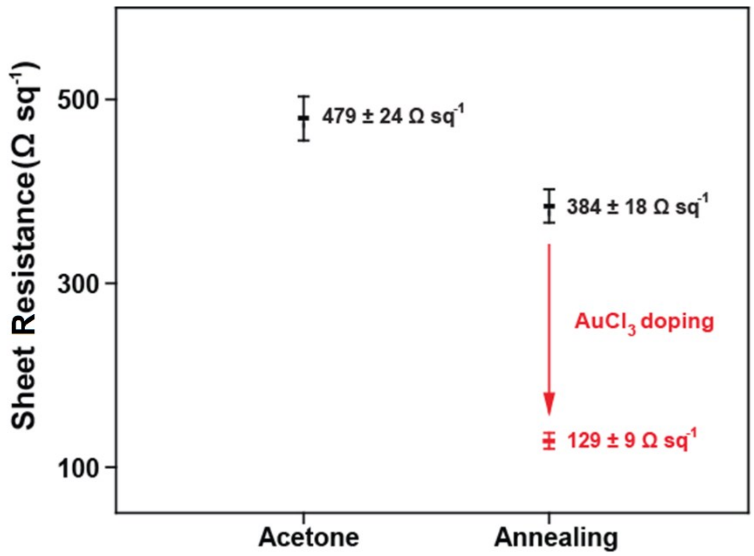

Fig. S4 Sheet resistance of the transferred graphene on SiO_2/Si substrate through various treatments performed in this work. The sheet resistance of acetone- and annealing-processed graphene is 479±24 and 384±18 Ω sq^{-1}, respectively. After doping with $AuCl_3$, the sheet resistance of graphene is further decreased from 384±18 to 129±9 Ω sq^{-1}.

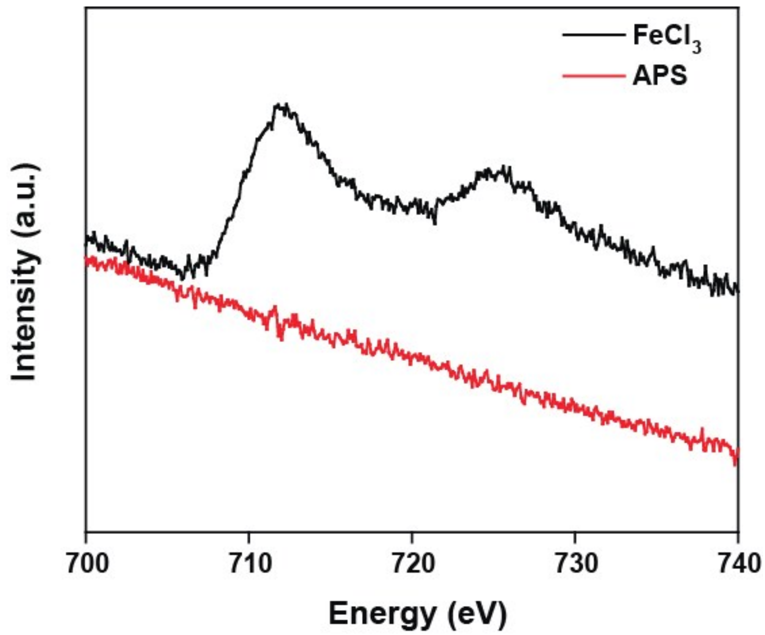

Fig. S5 XPS spectra of $FeCl_3$- and APS-transferred graphene. Fe 2p spectra of $FeCl_3$-transferred graphene indicate the existence of metallic impurity residues on the graphene surface.

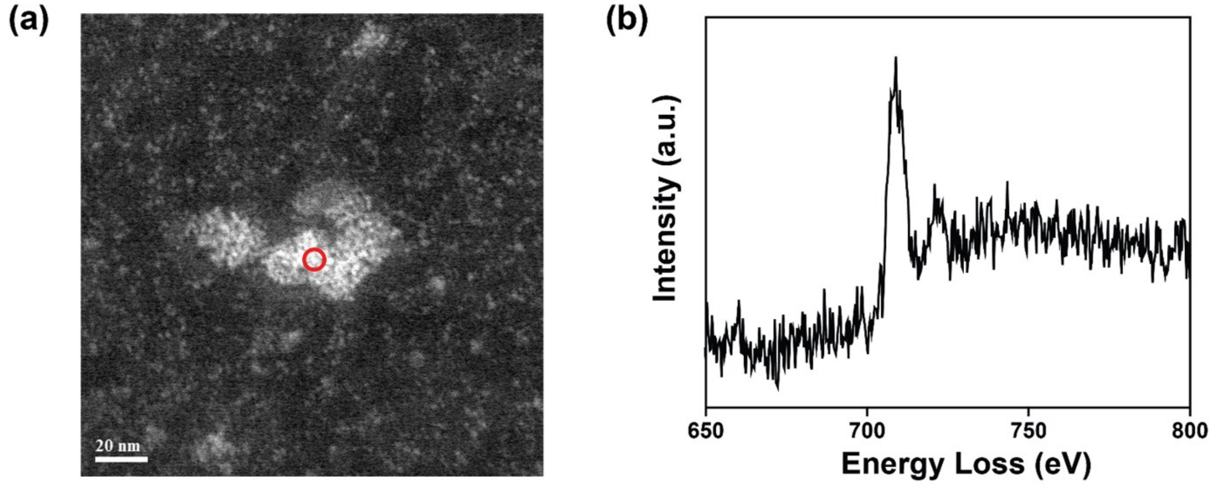

Fig. S6 Observation of metallic impurities by TEM. (a) TEM image of $FeCl_3$-transferred graphene and (b) EELS analysis on the particle clusters marked by red circle in (a).

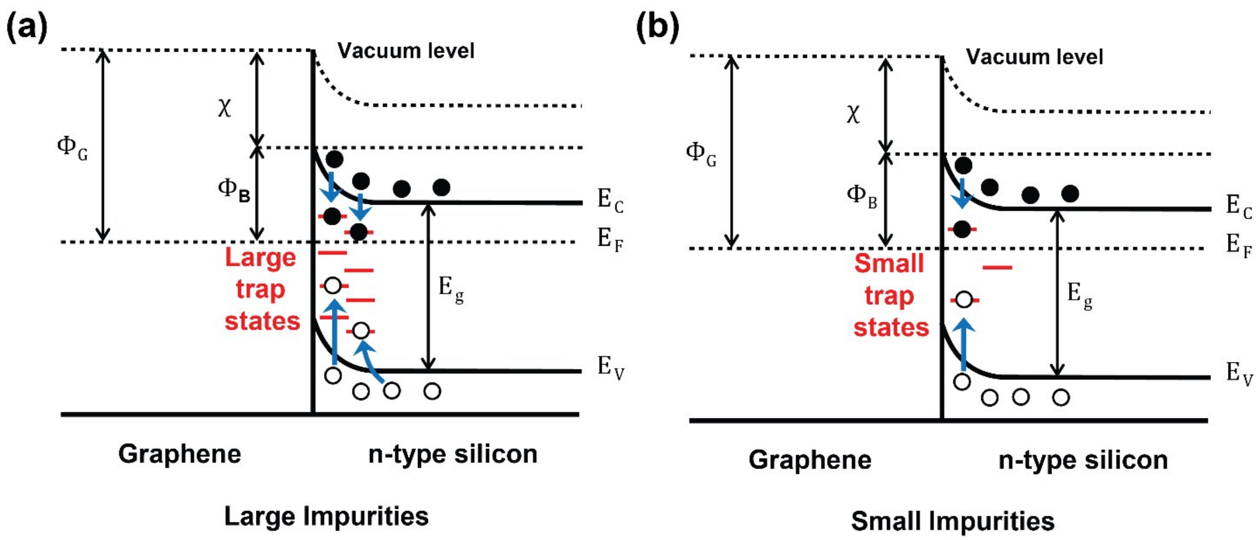

Fig. S7 Schematic energy band diagram of graphene-silicon Schottky junction with interface impurities. (a) Large impurities at graphene and silicon heterojunction generate more trap states leading to enhanced recombination of photogenerated electrons and holes compared to the (b) small impurity case.

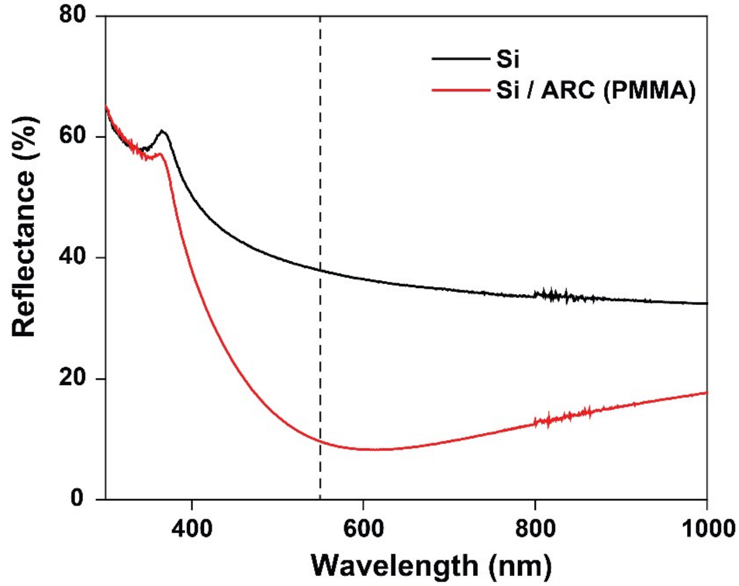

Fig. S8 Reflection spectra of bare silicon (black) and PMMA ARC-applied silicon (red). At 550 nm of wavelength (dashed line), reflectance of bare silicon and PMMA ARC-applied silicon is 38.0% and 9.6%, respectively.

Copper etching	PMMA removal	Doping	J_{sc} (mA cm^{-2})	V_{oc} (V)	FF (%)	PCE (%) max./avg.
APS	Acetone	Undoped	8.1 ± 3.0	0.34 ± 0.07	17.9 ± 3.7	0.8/0.5
		Doped	25.3 ± 2.8	0.50 ± 0.01	36.9 ± 4.7	5.5/4.7
	Annealing	Undoped	22.3 ± 1.6	0.35 ± 0.01	32.5 ± 2.6	2.8/2.6
		Doped	27.4 ± 2.4	0.51 ± 0.02	65.8 ± 3.8	9.5/9.1
$FeCl_3$	Acetone	Undoped	11.1 ± 4.3	0.34 ± 0.08	18.3 ± 3.4	1.1/0.9
		Doped	25.6 ± 1.0	0.46 ± 0.05	32.3 ± 5.9	4.7/3.7
	Annealing	Undoped	23.9 ± 1.9	0.36 ± 0.01	34.8 ± 3.6	3.9/3.1
		Doped	26.6 ± 2.1	0.47 ± 0.02	60.9 ± 4.4	8.5/7.6

The average values were obtained from at least 10 devices with standard deviations.

Table S1. Summary of device performance from graphene-silicon Schottky junction solar cells fabricated through various configurations of graphene integration processes: copper etching, PMMA removal, and doping.

	J_{sc} (mA cm^{-2})	V_{oc} (V)	FF (%)	PCE (%)
Pristine	23.8	0.35	33.4	2.8
Doping	29.0	0.51	64.0	9.5
Doping, ARC	37.0	0.53	63.3	12.5

Table S2. Summary of device performance from optimized graphene-silicon Schottky junction solar cells with $AuCl_3$ doping and PMMA ARC layer. Graphene films were prepared through APS and annealing processes.